Cyclic Spectral Analysis of Power Line Noise in the 3-200 kHz Band

Karl F. Nieman†, Jing Lin†, Marcel Nassar†, Khurram Waheed‡, and Brian L. Evans†
†The University of Texas at Austin, Austin, TX
‡Freescale Semiconductor, Inc., Austin, TX
Email: {karl.nieman, jing.lin, mnassar}@utexas.edu, khurram.waheed@freescale.com, bevans@ece.utexas.edu

***Abstract*—Narrowband OFDM Power Line Communication (NB-OFDM PLC) systems are a key component of current and future smart grids. NB-OFDM PLC systems enable next-generation smart metering, distributed control, and monitoring applications over existing power delivery infrastructure. It has been shown that the performance of these systems is severely limited by impulsive, non-Gaussian additive noise. A substantial component of this noise has time-periodic statistics (i.e. it is cyclostationary) synchronous to the AC mains cycle. In this work, we analyze the cyclic structure of power line noise observed in a G3 PLC system operating in the CENELEC 3-148.5 kHz band. Our contributions include: (*i*) the characterization of noise measurements in several urban usage environments, (*ii*) the development of a cyclic bit loading method for G3, and *(iii)* the quantification of its throughput gains over measured noise. Through this analysis, we confirm strong cyclostationarity in power lines and identify several sources of the cyclic noise.**

I. Introduction

Future smart grids use an intelligent network of sensors and distributed control to improve the reliability and efficiency of power generation and distribution. One key component of these networks are Narrowband Orthogonal Frequency Division Multiplexing Power Line Communication (NB-OFDM PLC) systems. NB-OFDM PLC systems communicate using high frequency, digitally-modulated signals that are coupled into power lines and transmitted across the grid. These systems operate in the 3-500 kHz band and can achieve data rates of up to several hundred kbps at up to several km range. This allows the formation of digital communication networks over existing power delivery infrastructure. See [1] for a detailed summary of the state-of-the-art in NB-OFDM PLC.

One of the primary impairments for communications in NB-OFDM PLC is impulsive, non-Gaussian additive noise. This noise has periodic temporal and spectral properties and can be modeled as a cyclostationary random process [2]. In [3] the noise is modeled as a Gaussian distribution whose variance is a continuous and periodic function of time. The authors in [4] model the noise as a linear periodic time-varying system – i.e. a filter bank that shapes white Gaussian input noise to different spectral shapes and powers with selectable outputs. These shaped noise outputs are individually selected during subintervals of half the AC mains period. Field data was fit closely using a three filter configuration.

K. Nieman, J. Lin, M. Nassar, and B. L. Evans are supported by the GRC Program of the Semiconductor Research Corporation under Task ID 1836.063.

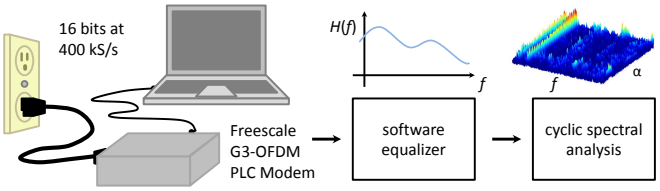

Fig. 1. The measurement setup consists of Freescale's PLC G3-OFDM modem connected to a power outlet controlled using a laptop over USB2.0. Analysis is performed on equalized line samples using MATLAB.

In this work, we apply cyclic spectral analysis techniques developed in [5] to quantify the strength and coherence of the cyclostationary components of power line noise samples in the CENELEC band shown in Table I. These methods allow us to decompose the noise power spectral density into its periodic components and evaluate its adherence to a periodic structure using a coherence measure. The analysis is performed on noise samples collected using the test setup shown in Figure 1.

II. Background

Current electric grids were designed for power delivery at the AC mains frequency, making them a less than ideal medium for digital communications. Noise present in NB-PLC bands can be attributed to switching loads and generation sources attached to the grid. Sources of synchronous noise can include semiconductor controlled rectifier (SCR)-based light dimmers and motor controllers that power loads on and off at different phases of the AC cycle. Other switching circuits such as DC-DC converters can contribute asynchronous but periodic noise into power lines. The authors of [6] analyze the broadband noise emissions of different loads in an anechoic chamber using a 100 MS/s sampling system. They observe strong cyclic noise properties, particularly for loads with high current AC motors and/or SCR switching devices.

TABLE I
CENELEC Bands for NB-OFDM PLC

Designation	A	B	C	D
Band (kHz)	3-95	95-125	125-140	140-148.5

A. NB-PLC Noise Sources

Additive powerline noise is generated by electrical devices connected to the power grid, and by external noise and interference coupled to the power network via radiation and/or conduction. In the 3–500 kHz band, the powerline noise can generally be decomposed into four classes [7]:

1) *Spectrally-shaped background noise*. The background noise is the summation of numerous low-power noise sources. Its power spectral density slowly varies over time (in minutes or even hours), and exhibits a $1/f$-type decay due to the decreasing concentration of noise sources with frequency.
2) *Cyclostationary noise*. The cyclostationary noise exhibits cyclostationarity in both the time and the frequency domain, with period equal to half or one AC cycle [8]. It typically appears in one of the two forms:
   a) *Periodic impulsive noise synchronous to the mains frequency*. This type of noise consists of a series of isolated impulses of considerable duration and amplitude. The impulses have a repetition rate of 60/120 Hz (in the US) and always appear at the same instant of the AC cycle. They are typically caused by nonlinear power electronic devices, such as silicon controlled rectifiers and diodes, that switch on and off with the AC cycle while generating abrupt switching transients.
   b) *Periodic impulsive noise asynchronous to the mains frequency*. This noise component takes the form of impulse trains with repetition rates unrelated to the mains frequency [9]. In addition to the high repetition frequencies, it also exhibits an underlying period equal to half the mains cycle. It is primarily injected by switching mode power supplies that operate at frequencies above 20 kHz. The impulses in such noise typically have much lower amplitudes and shorter durations than those in the synchronous impulsive noise, and hence are usually masked by other high-level noise components in the time domain. In the frequency domain, however, such noise can be easily identified as evenly spaced harmonic clusters with significantly higher power spectral density over the background noise.
3) *Narrowband interference*. Broadcast stations in the long-wave bands (153–279 kHz) introduce narrowband interference in NB-OFDM PLC systems. The interference exhibits amplitude or frequency modulated sinusoids in the time domain, which correspond to harmonic clusters in the noise spectrum. The interference level generally varies slowly with daytime, and in some cases varies periodically with half the AC cycle, i.e., is cyclostationary.
4) *Asynchronous impulsive noise*. This type of noise consists of impulses of significant duration and amplitude. It typically arises from switching transients caused by the connection and disconnection of electrical devices.

Recent field measurements on outdoor medium-voltage and low-voltage power lines have shown that cyclostationary noise, including periodic impulsive noise synchronous and asynchronous to the mains frequency, is the dominant noise component in the 3–500 kHz band [4].

B. Cyclic Spectral Analysis

Cyclostationary signals are a special class of non-stationary random processes that have a periodic *instantaneous auto-correlation function* $R_{XX}[n,l]$ such that

$$R_{XX}[n,l] = R_{XX}[n+kN,l], \quad \forall k \in \mathbb{Z} \tag{1}$$

where we define the *symmetric instantaneous auto-correlation function* of random process X as

$$R_{XX}[n,l] = \mathbb{E}\left\{ X\left[n+\frac{l}{2}\right] X^*\left[n-\frac{l}{2}\right]\right\}. \tag{2}$$

These cyclostationary processes have periodic second-order statistics that define their distribution as a function of time; therefore, the periodicity implied by (1) lends $R_{XX}[n,l]$ to be represented as a Fourier series

$$R_{XX}[n,l] = \sum_{\alpha_i \in \mathscr{A}} R_{XX}\left[l,\alpha_i\right] e^{j2\pi\alpha_i n\Delta} \tag{3}$$

where $\mathscr{A} = \{\alpha_i\}$ is the set of cyclic frequencies α_i. By the additional application of a Fourier transform to the time-dimension n of $R_{XX}[n,l]$, this cyclic auto-correlation function can be transformed to yield a 2-D function of cyclic frequency α and frequency f:

$$\mathscr{S}(\alpha,f) = \Delta^2 \sum_{n=-\infty}^{\infty}\sum_{l=-\infty}^{\infty} R_{XX}\left[n,l\right] e^{-j2\pi\alpha n\Delta} e^{-j2\pi f l\Delta}. \tag{4}$$

Finally, we define the symmetric cyclic coherence function as:

$$\mathscr{C}_{YX}(f;\alpha) = \frac{\mathbb{E}\left\{ \mathrm{d}Y\left(f+\frac{\alpha}{2}\right) \mathrm{d}X\left(f-\frac{\alpha}{2}\right)\right\}}{\sqrt{\mathbb{E}\left\{\left|\mathrm{d}Y\left(f+\frac{\alpha}{2}\right)\right|^2\right\}\mathbb{E}\left\{\left|\mathrm{d}X\left(f-\frac{\alpha}{2}\right)\right|^2\right\}}}. \tag{5}$$

Details about this method and its use can be found in [5].

For this study, three spectral analysis techniques are used. First, the noise samples are analyzed using a spectrogram which shows the evolution of the signal power spectral density as a function of time. The spectrogram is computed using a 512-point FFT with a 256-length Hamming window with an overlap of 170 samples. Second, the samples are processed using a discrete-time implementation of (4) with the same settings as above. The cyclic frequencies examined are bins 1 through 150 (indexing by zero) corresponding to cyclic frequencies of 25 Hz to 3750 Hz with a 25 Hz step size. A discrete time implementation of equation (5) is then used with the same settings. The results path two and three are then sinc-upsampled by a factor of 8 to provide a smaller mesh size for visualization. The results from the first, second, and third parts of this analysis are displayed in parts (a), (b), and (c) of the figures shown in Section III.

III. Case Studies

Noise from several usage scenarios was collected and analyzed using Freescale's PLC G3-OFDM modem. The modem was configured to capture 16000 16-bit line samples at 400 kS/s. These samples were then equalized in the frequency domain using coefficients derived from a calibration procedure via the zero-forcing solution to a received 16000 chirp sequence. The noise samples collected during this work and the software used to analyze them are available for download: http://www.ece.utexas.edu/~bevans/papers/2013/PLCcyclic/

A. Office Space (ENS 414D)

Noise samples for case study *A* were collected at an outlet in a student office area on the fourth floor of the Engineering Sciences (ENS) Building located at The University of Texas at Austin. Nearby electronic devices connected to the power system are primarily desktop workstations and monitors and overhead fluorescent bulbs. Figure 2(a) shows the spectrogram of the noise, which shows the dominant components of the noise are a collection of narrowband noise sources between 60 and 70 kHz. Additionally, there is an impulsive (broad spectrum, short temporal support) noise emission from DC to 30 kHz that repeats every 8.3 ms (half the AC mains cycle). It is also observed that there is a repeating broad spectral and temporal noise from DC to 30 kHz between the impulses. Additionally, there is a weak narrowband emission at 140 kHz.

Figure 2(b) displays the spectral density as a function of the cycle frequency α, and Figure 2(c) shows its cyclic spectral coherence. As seen in these two plots, the impulsive components from DC to 30 kHz are transformed into a Fourier series that is also an impulse train with 120 Hz (twice the AC mains frequency) spacing. The high coherence measure of ~0.7 reveals that the noise at these frequencies are strongly cyclic and are actually composed of two components, one ~10 kHz and one ~30 kHz. The narrowband interference between 60 and 70 kHz has roughly the same power density as a function of cycle frequency and has a low coherence, revealing that it is not periodic. The narrowband noise source at 140 kHz has an impulse-like cyclic coherence function at 120 Hz, revealing that its instantaneous autocorrelation is highly sinusoidal as a function of time at that frequency.

B. Laboratory (ENS 607)

Figure 3 displays the results of the analysis on noise samples collected on the sixth floor of the ENS Building in laboratory space ENS 607. Nearby components connected to the power lines include overhead fluorescent light fixtures, a function generator, an oscilloscope, and other electronic hardware. On the same floor, there are adjacent laboratories with similar equipment. As we see in Figure 3(a), there are several narrowband noise sources from 65-80 kHz which appear to be modulated at half the AC mains period and at a higher frequency. Impulsive noise bursts spanning 20-60 kHz can be seen in the time samples, five of which are periodic at 120 Hz (the fifth is located on the far right portion of the plot) and two of which appear aperiodic (impulses at 20 and 37 ms).

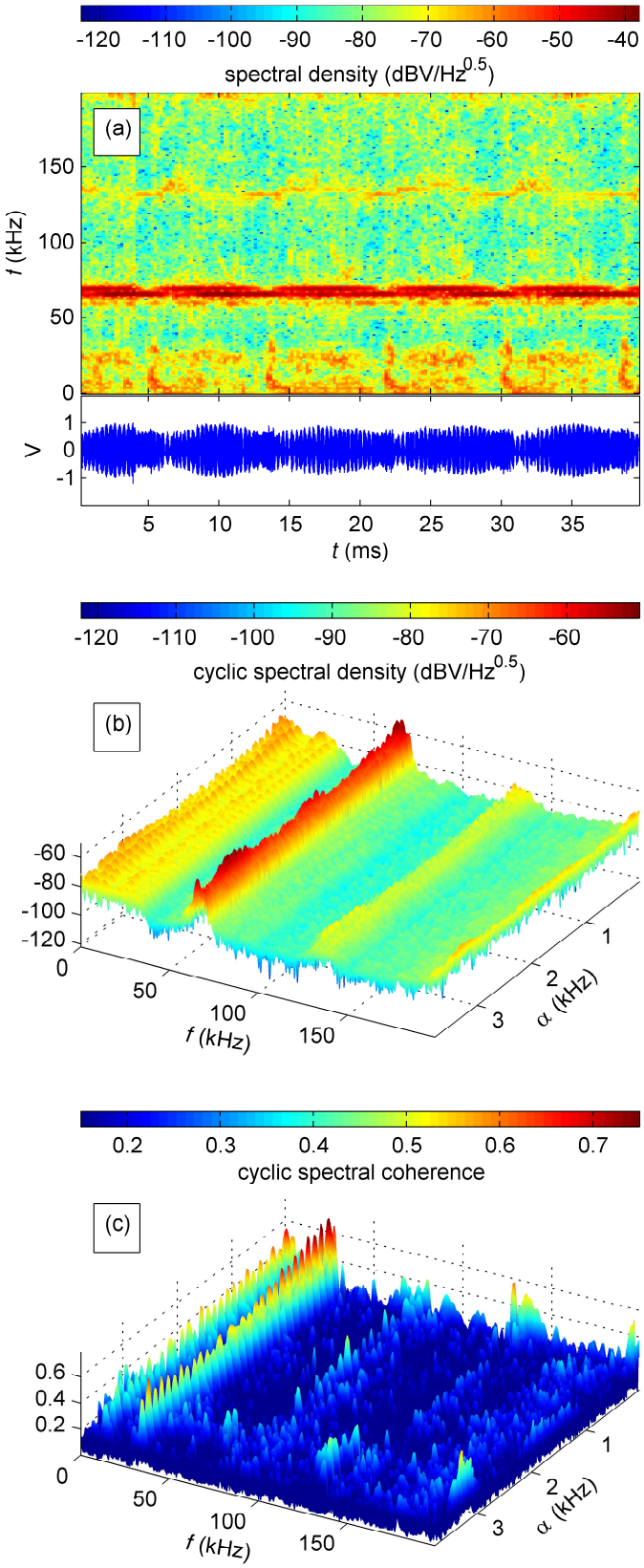

Fig. 2. Analysis of noise samples collected in ENS 414D, a student office space: its (a) normalized spectrogram and noise samples, (b) cyclic power spectrum, and (c) cyclic spectral coherence. The predominant noise source is several non-cyclostationary narrowband sources in 60-70 kHz and an impulse followed by broad noise in the DC to 30 kHz range.

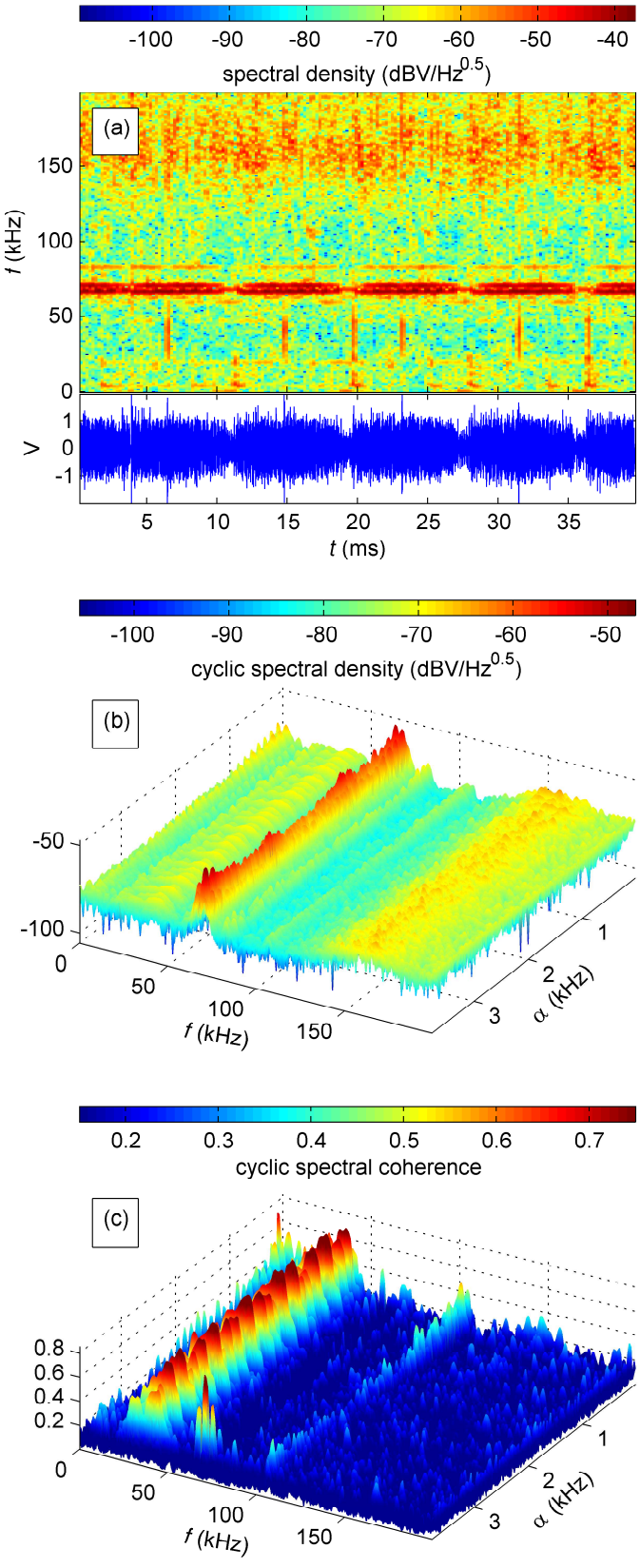

Fig. 3. Analysis of noise samples collected in ENS 607, a laboratory space with nearby electronic instrumentation: its (a) normalized spectrogram and noise samples, (b) cyclic power spectrum, and (c) cyclic spectral coherence. The predominant noise source consists of several narrowband sources at 60-70 kHz and 80 kHz and impulses in the 20-60 kHz frequency range.

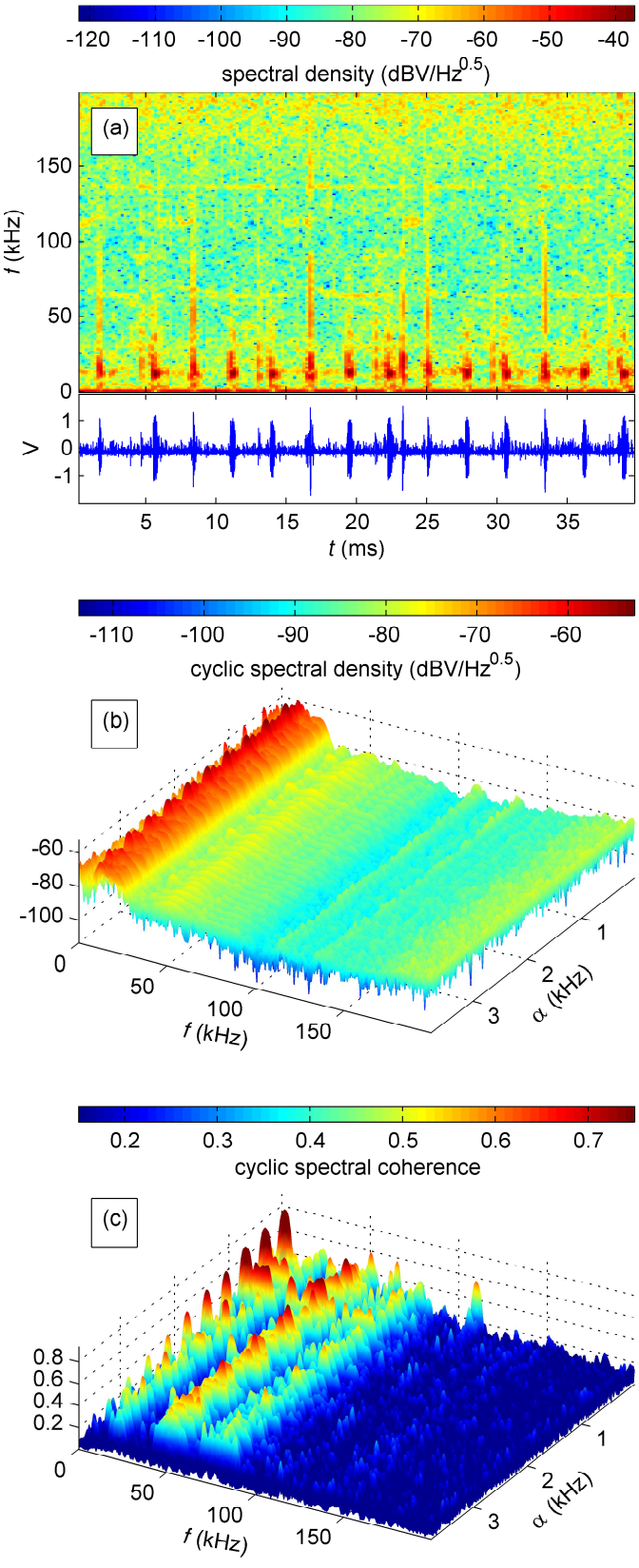

Fig. 4. Analysis of noise samples collected at the Hal C. Weever Power Plant/Chilling Station: its (a) normalized spectrogram and noise samples, (b) its cyclic power spectrum, and (c) its cyclic spectral coherence. The dominant noise sources are periodic impulses from DC to 30 kHz with additional impulses from DC to 100 kHz repeating every 8.3 ms.

Examination of Figures 3(b) and 3(c) reveals several strong periodic structures with cyclic frequency α of 120 Hz. The first has an impulse-like coherence at $f = 600$ Hz and others at $f = 60$, 71, and 150 kHz. The narrowband noise at $f = 67.5$ kHz is shown to be strongly cyclic with $\alpha = 3.675$ kHz. This is likely caused by fluorescent lighting ballasts.

C. Industrial (Hal C. Weever Power Plant/Chilling Station)

For case study *C*, noise samples were collected at an outdoor outlet connected to a large industrial power plant and water chilling station located at UT campus on the south side of 24th Street between Speedway and San Jactinto. The characteristics of this noise are vastly different from that of *A* and *B*. As seen in Figure 4(a), the noise trace consists of a number of short impulsive bursts that have both periodic and aperiodic components. Most of the noise power is concentrated between DC and 30 kHz with a weak narrowband noise source at 65 kHz and another at 110 kHz and 140 kHz.

The cyclic spectral analysis in Figures 4(b) and 4(c) show that the impulsive noise bursts <30 kHz have periodic components at $\alpha = 360$ Hz, or six times the AC mains frequency. The impulses with power in from DC to 90 kHz are periodic with period equal to half the AC cycle. The noise source at 140 kHz does not appear to have periodic second order statistics.

D. Residential

For case study *D*, noise samples were collected in the living room of an apartment in central Austin, TX. The apartment is part of a two story building with 16 units and is lit using compact fluorescent bulbs. Figure 5(a) reveals a large number of noise sources with various spectral and temporal properties. The remaining noise sources vary in spectral shape, but all appear to be periodic with a predominant period of 8.3 ms.

As shown in Figure 5(b) and 5(c), the noise at frequencies 4, 45, 58-70, 75, 80-85, 90-120, and 133-140 kHz are all periodic with twice the AC frequency. A noise source at 166 kHz is periodic at four times the AC frequency. The large asynchronous impulse at t = 14 ms with spectral support from 10-14 kHz produces a long streak in the coherence over all α.

IV. Adaptive Rate/Modulation for Communication in Cyclostationary Noise

The system settings of Table II reveal that G3-PLC OFDM frames can span many AC cycles. G3 currently supports static modulation with tone map over an OFDM frame. The large spectral and temporal variations of noise power over that duration and the cyclic nature of the noise imply that a cyclic bit loading scheme could be used to improve system throughput. Adaptive bit loading has been proposed for PLC [10] and could be tailored to cyclic noise.

Using noise trace from case study *D*, we consider an adaptive modulation scheme for a G3 system operating in the CENELEC-A band (see Figure 6(a)). We assume that this scheme could be supported using an expanded tone map message that specifies a cyclic bit loading map to the transmitter. The tone map message would need to be a 36 ×

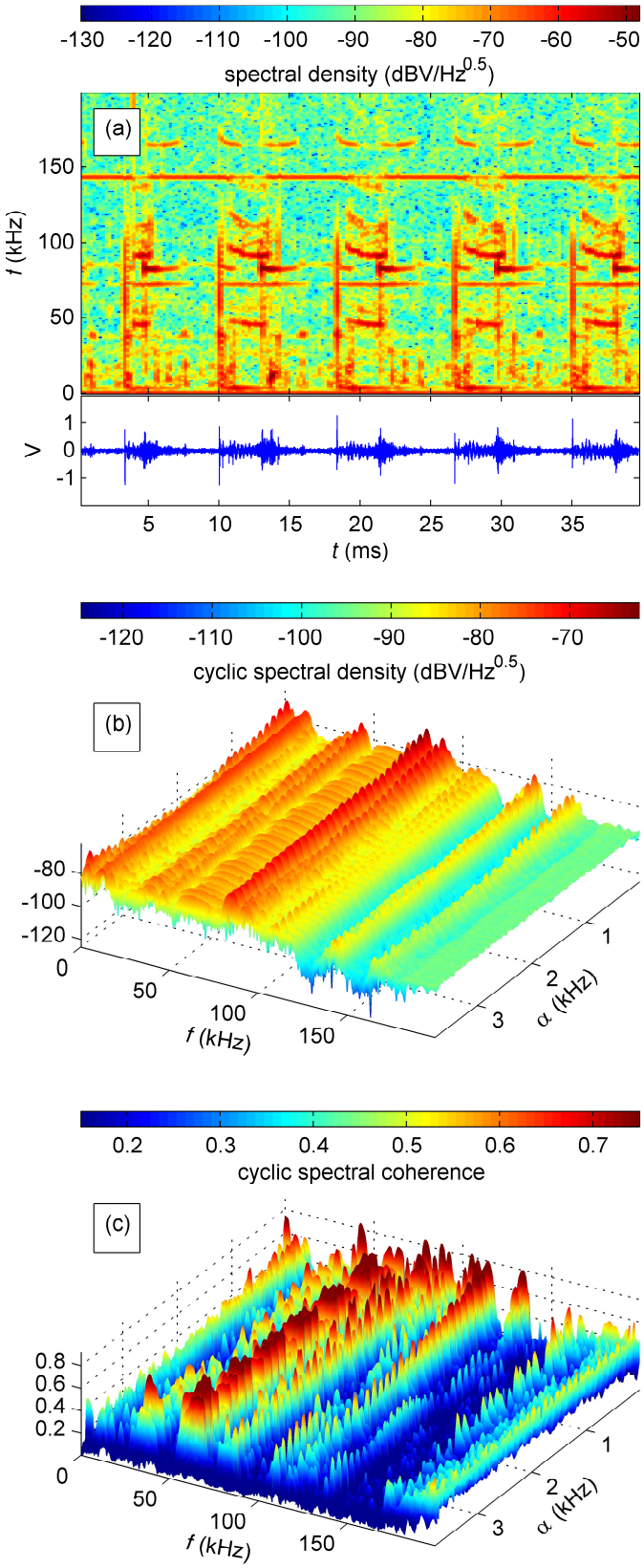

Fig. 5. Analysis of noise samples collected in the living room of an apartment in central Austin, TX: (a) its normalized spectrogram and noise samples, (b) its cyclic power spectrum, and (c) its cyclic spectral coherence. A large number of narrowband and impulsive noise sources are observed, many of which are cyclical with an 8.3 ms period.

TABLE II
FREESCALE NB-OFDM PLC SYSTEM SETTINGS

Number of FFT points	N = 256
Number of overlapped samples	N_O = 8
Number of cyclic prefix samples	N_{CP} = 30
Sampling frequency	f_s = 0.4 MHz
Subcarriers used	23-58
OFDM frame length	~15-190 ms

12 (subcarrier $\times$ symbol) field of 3 bits entries that specify the modulation to use for half the AC cycle (~12 symbols for 60 Hz and ~10 for 50 Hz). This message could be exchanged during link negotiation based on noise sampled at the receiver during quiet time (arising from the bursty nature of NB-PLC transmissions). We focus solely on the effect of additive noise in an uncoded link with target bit error rate (BER) 10^{-2} using the configuration in Table II. A further study could take into account the effects of channel, coding, and link delay.

The modulation schemes currently supported in G3 from most robust to highest throughput are ROBO (4x repetition-coded DBPSK signal), DBPSK, DQPSK, and D8PSK. Figure 6(b) shows the highest decodable modulation from this set for each OFDM symbol and subcarrier based on the noise present throughout the OFDM frame (see Figure 6(a)). Figure 6(c) compares the throughput of static modulation allocations with tone mask versus a cyclic adaptive modulation scheme based on the observations of the first 12 symbols (corresponding to ~half the AC cycle). A tone mask is applied to disable tones that do not meet the SNR threshold of a given modulation (i.e. theoretical BER $\leq 10^{-2}$) for at least half the OFDM frame duration. This causes the higher rate D8PSK to underperform the lower rate DQPSK. The cyclic adaptive modulation scheme approaches the optimal adaptive modulation scheme, which is displayed as a dashed line. Substantially higher gains could be realized with a larger modulation set.

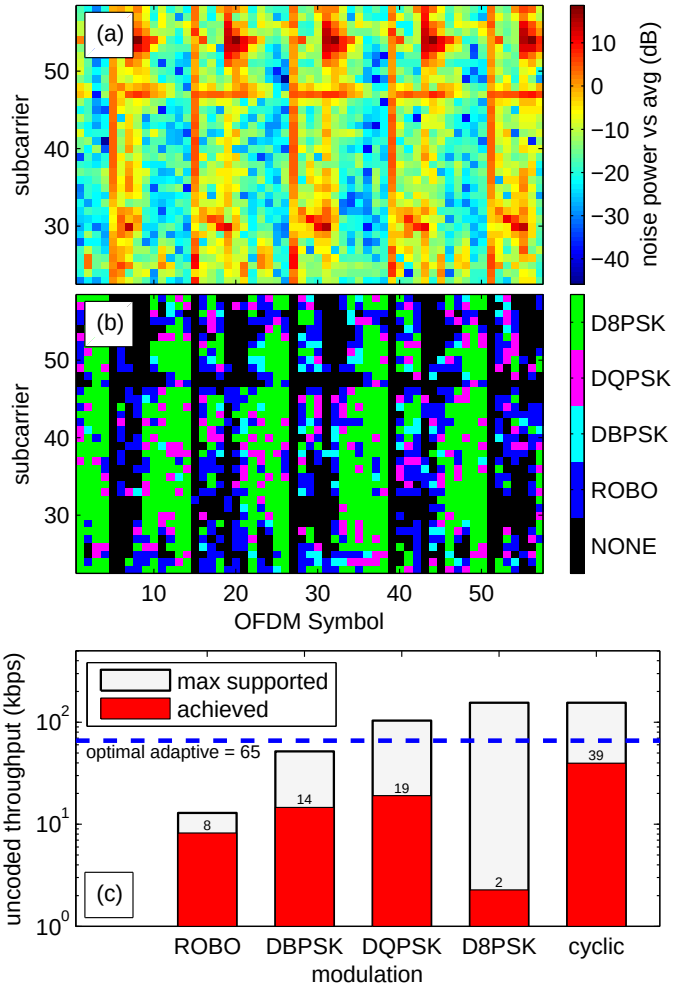

Fig. 6. Adaptive modulation for G3 operation in CENELEC-A band using noise trace from case study *D* with TX Power = $\mathrm{SNR}_{\mathrm{avg}}$ - 7 dB: (a) noise power across an OFDM frame, (b) optimal G3 modulation allocation, and (c) throughput for static modulations with tone mask and the proposed cyclic loading scheme. The optimal modulation allocation is displayed as a dash and achieved throughput in kbps is shown at the top of each bar.

V. CONCLUSION

In this work, we have characterized power line noise at several usage locations. It is confirmed that the noise at each location is predominantly cyclostationary with dominant period equal to half the AC cycle. Other noise such as asynchronous impulsive noise and narrowband noise are observed. We demonstrate the utility of implementing an adaptive cyclic modulation scheme for G3-PLC operation in the CENELEC-A band using measured noise samples. Our results show that this scheme is capable of offering up to a 2$\times$ increase in throughput using the current G3 modulation set.

REFERENCES

[1] M. Nassar, J. Lin, Y. Mortazavi, A. Dabak, I. H. Kim, and B. L. Evans, "Local utility powerline communications in the 3-500 khz band: Channel impairments, noise, and standards," *IEEE Signal Process. Mag.*, vol. 29, no. 5, pp. 116–127, 2012.

[2] W. Gardner and L. Franks, "Characterization of cyclostationary random signal processes," *IEEE Trans. Inf. Theory*, vol. 21, no. 1, 1975.

[3] M. Katayama, T. Yamazato, and H. Okada, "A mathematical model of noise in narrowband power line communication systems," *IEEE J. Sel. Areas Commun.*, vol. 24, no. 7, 2006.

[4] M. Nassar, A. Dabak, I. H. Kim, T. Pande, and B. L. Evans, "Cyclostationary noise modeling in narrowband powerline communication for smart grid applications," *Proc. IEEE International Conference on Acoustics, Speech, and Signal Processing*, 2012.

[5] J. Antoni, "Cyclic spectral analysis in practice," *Mechanical Systems and Signal Processing*, no. 21, pp. 597–630, 2007.

[6] S. Güzelgöz, H. B. Celebi, T. Guzel, H. Arslan, and M. C. Mihcak, "Time frequency analysis of noise generated by loads in PLC," *Proc. IEEE International Conference on Telecommunications*, 2010.

[7] M. Zimmermann and K. Dostert, "Analysis and modeling of impulsive noise in broad-band powerline communications," *Electromagnetic Compatibility, IEEE Transactions on*, vol. 44, no. 1, pp. 249 –258, 2002.

[8] S. Barmada, A. Musolino, and M. Tucci, "Response bounds of indoor power-line communication systems with cyclostationary loads," *Power Delivery, IEEE Transactions on*, vol. 24, no. 2, pp. 596 –603, april 2009.

[9] M. H. L. Chan and R. W. Donaldson, "Amplitude, width, and interarrival distributions for noise impulses on intrabuilding power line communication networks," *Electromagnetic Compatibility, IEEE Transactions on*, vol. 31, no. 3, pp. 320 – 323, 1989.

[10] N. Sawada, T. Yamazato, and M. Katayama, "Bit and power allocation for power-line communications under non-white and cyclostationary noise environments," *Proc. IEEE International Symposium on Power Line Communication and Its Applications*, 2009.